Advances in Science and Technology Research Journal

Advances in Science and Technology Research Journal, 2025, 19(1), 197–208
https://doi.org/10.12913/22998624/195002
ISSN 2299-8624, License CC-BY 4.0

Received: 2024.08.27
Accepted: 2024.11.15
Published: 2024.12.01

Disturbances in-situ measurement results on the example of heat transport in multilayer building walls

Arkadiusz Urzędowski[1*], Agnieszka Gandzel[1], Andrzej Sachajdak[2], Paśnikowska-Łukaszuk[1]

[1] Faculty of Mathematics and Information Technology, Lublin University of Technology, Nadbystrzycka 38, 20-618 Lublin, Poland

[2] Faculty of Energy and Environmental Engineering, Silesian University of Technology, Stanisława Konarskiego 18, 44-100 Gliwice, Poland

ABSTRACT

The paper demonstrates the challenges in accurately measured heat transport through multilayer walls, emphasizing the need for careful sensor placement and analysis to address potential anomalies and ensure reliable data. The study was conducted on a building constructed in 2010 for agricultural purposes in rural region. The structure, with dimensions of 6×16.8 meters and a single-pitched roof, has partial basement and lacks insulation. The external wall, facing northeast, has internal dimensions of 5.5×3.0 meters and a peak height of 7.5 meters, and is made of 0.24 m thick aerated concrete blocks. The experiment involved placing thermocouples in the walls before installing thermal insulation, with one model coated with a reflective smoothing layer. In the first case, inside the building, the issue was identified as a failure to record data from one channel due to sensor damage, which was detected after the research was completed. In the second case, an error recorded outside was caused by the placement of a temperature sensor in close proximity to a thermal bridge, which distorted the readings. The diagnosis was made possible after processing the results. A large dataset, consisting of nearly 5E6 readings, was collected, which detailed analysis of the graphical and time-consuming interpretation of the results enabled proper interpretation and conclusions. Algorithms based on artificial intelligence could be successfully used to conduct such analyses and detect errors at an early stage of research. These algorithms can perform multicriteria analysis of recorded data in real-time which is of fundamental importance when carrying out research that is not dynamic and requires a long observation time, i.e. during changes in the external temperature.

Keywords: heat measurements, building walls, in-situ methods.

INTRODUCTION

Improving the energy efficiency of existing buildings to meet new sustainability goals is a significant challenge [1]. Accurate estimation of wall thermal transmittance is crucial for implementing effective energy conservation measures [2, 3]. The variety of available methods to determine overall heat transfer coefficients and the absence of a comprehensive review of these methods for calculating U-values, a thorough review is necessary [4, 5, 6, 7, 8]. Proper insulation can significantly reduce the energy requirements for cooling and heating systems by minimizing unauthorized heat gain or loss [9, 10, 11]. Worldwide awareness of energy conservation requirements has been increasing in recent years. For this reason, measures are taken to limit heat loss through a building envelope and its internal partitions. The search for materials with increasingly better insulating properties is being continued [12]. There is a need to verify these properties. The paper discusses the measurement methods of thermal conductivity specific for building materials and the heat transfer coefficient through building partitions in situ conditions.

Measurement errors

The ability to properly process measurement results is essential in many fields of science, technology, and the economy. The high importance of this issue is evidenced by the work of international committees, whose goal is to find and standardize methods for processing measurement results [13]. In general, errors are classified into: systematic, random, gross (excessive). The final measurement result should be a corrected result, i.e., it should not include known systematic and gross errors [14].

Systematic errors can be divided into: constant systematic and variable systematic errors. A constant systematic error can be detected by repeating the measurement experiment under deliberately altered (modified) physical conditions. If the results of a repeated measurement experiment in an apparently unchanged set of physical conditions exhibit systematic variation (drift), then the measurement results are subject to variable systematic error. This type of error arises, for example, due to changes in a dominant interfering (influencing) quantity, such as the ambient temperature. The presence of variable systematic error indicates that the fundamental set of physical conditions of the measurement experiment is not constant [15]. In the analysed experimental results within this paper, measurement uncertainty related to atmospheric condition changes can be observed, however they are spread over time and do not affect the observed correlations.

Random errors occur when repeating the measurement experiment in an apparently unchanged set of physical conditions reveals random variability in the results. The word "apparently" is particularly significant in this context because random errors are caused by the interaction of many variables, which are generally independent of each other. Some precise deterministic description of such interactions is rather a matter of unlinear dynamics and it exceeds the frames of this research. An example of a measurement dominated by random factors is the measurement of the instantaneous noise voltage of a resistor [16, 17]. Probabilistic models are used to describe random errors.

Gross errors can be caused by reading errors, temporary strong disturbances, or other factors. The simplest approach is to discard results that differ significantly from the expected values. A more appropriate method is to apply a suitable statistical test [18]. In-situ testing is associated with greater errors compared to laboratory testing; however, it is essential because it provides the information necessary for the validation and verification of digital models, enabling the conduct of multi-scenario, non-destructive analyses [19, 20, 21]. Errors in heat measurements in walls can also be caused by issues with thermocouples [22].

Determination of thermal parameters of multilayer walls

Thermal conductivity coefficient characterizes the intensity of heat exchange through a given material. It defines the amount of energy (expressed in watts) that passes through one square meter of a building element (such as a wall, roof, window, or door) when there is a temperature difference of 1 K (Kelvin) across it. *U* value affects the amount of thermal energy flowing from the warm side to the cold side for a given mass of the sample, due to an external temperature difference [9, 23]. For a body with a rectangular parallelepiped shape conducting heat under steady-state conditions, the amount of heat transferred through this body depends on the type of substance and is also proportional to the cross-sectional area of the body, the temperature difference between the surfaces perpendicular to the direction of heat flow, and the duration of heat flow, what can be expressed by the formula 1:

$$\mathrm{Q} = \lambda \cdot \frac{S \cdot \Delta T \cdot t}{d} \tag{1}$$

where:

$$\lambda = \frac{Q}{t} \cdot \frac{d}{S \cdot \Delta T} \tag{2}$$

where: λ–thermal conductivity [W/(m·K)], Q–the amount of heat flowing through a body [J], t– duration of heat flow [s], S–cross-sectional area of the body [m^2], ΔT–temperature difference along the direction of heat conduction [K], d – wall thickness [m].

The lower the value of the thermal conductivity coefficient (λ), the thinner the barrier can be while still achieving the required values specified in standards such as Technical Conditions [24]. This has a significant impact on construction costs. For investors, it may also be important to verify whether the declared thermal conductivity coefficient is as stated by the manufacturer. Interior parameters result in greater than expected heat losses, leading to higher building operating costs.

The thermal resistance of a building partition depends on the thermal conductivity coefficients λ of the materials from which it is constructed and the thicknesses d of the layers. For a uniform layer, this can be expressed as 3:

$$R = \frac{d}{\lambda} \tag{3}$$

The standard PN-EN ISO 6946 [25] defines the total thermal resistance R_T of a building partition, consisting of thermally homogeneous layers, perpendicular to the direction of heat flow, as the sum of the heat transfer resistance at the interior surface R_{si}, the thermal resistances of each layer, and the heat transfer resistance at the exterior surface R_{se} (4):

$$R_T = R_{si} + R_1 + R_2 + \ldots + R_n + R_{se} \tag{4}$$

This implies that heat transfer coefficient (U-value) of the building component (5), is reverse to the sum of resistance and maximum allowable U values for walls, roofs, floors and ceilings are defined by national regulations and standards [26, 27].

$$U = \frac{1}{R_T} \tag{5}$$

In situ measurements

In situ research refers to a type of study conducted in the natural environment. It can be distinguished from ex situ research, which can be carried out indoor in a laboratory or in other controlled circumstances. In situ research is often utilized in fields such as environmental science and archaeology. Currently, there is no standardized method for conducting an in situ quantitative diagnosis of the thermal insulation of building walls. Several methods have been developed in the academic sphere, significant efforts are being made to enhance their accuracy, speed, and applicability [28, 29]. However, these methods are not yet sufficiently mature for widespread use [30].

In contrast, many experimental methods for measuring material thermal conductivity are now standardized. For the thermal insulation of building walls, only two standardized techniques are available: ISO 9869-1 [31] and ISO 9869-2 [32]. However, these methods often fail to accurately assess thermal resistance or U-value in many situations, particularly when heat transfers are not in a steady-state regime or when the indoor-outdoor temperature gradient is too small. This shortfall is mainly because these methods are passive and, therefore, strongly influenced by climatic conditions [4, 9, 33]. Thus, there is a need to perform experimental measurements and develop new in situ diagnostic methods that can be used under most conditions occurring under real-world. The primary objective of this study is to propose a procedure to estimate in situ heat losses over an entire wall surface. This method should account for the contributions of thermal bridges. The estimation of wall heat losses will be based on the knowledge of the global heat exchange coefficient [34]. In the article, a method for measuring thermal resistance and heat transfer coefficient was applied using a multi-channel temperature recorder, which distinguishes this research method. In other scientific studies, authors typically use commercially available devices for transient U-value measurement or conduct measurements using thermography [35, 36, 37]. These studies typically focus on a single measurement point, whereas in this work, measurements were conducted using 40 sensors simultaneously.

Solving thermal issues using AI

It is also recommended to consciously apply machine learning methods and artificial intelligence to identify correlations and detect measurement errors. One method that could contribute to verifying the accuracy of experiments is artificial neural network (ANN), currently a widely utilized method for predicting building energy and thermal behaviour [7, 38]. In building energy applications, ANNs are extensively applied for predicting energy consumption, indoor temperature, indoor thermal comfort, and other related parameters [39, 40, 41]. Furthermore, ANNs have been integrated into various computing software, such as MATLAB, which facilitates their use in research [42]. Another powerful tool gaining increasing popularity across various industries and scientific fields is machine learning (ML) [5]. Numerous powerful machine learning based semantic segmentation algorithms have emerged in recent years, which can assist in forecasting research outcomes and quickly verifying the occurrence of anomalies and measurement errors. Architectures such as U-Net [43], ConvNet [44], ResNet [45] and SWIN Transformer [46] have become prominent deep learning models. These networks leverage convolutional neural network (CNN) layers, which outperform fully connected layers in image segmentation tasks. This method utilized thermal images of road surfaces and exhibited minimal complexity, however the challenge in *in situ* research remains the training of AI algorithms under consistent, repeatable conditions [47, 38].

Measurement methodology

Figure 1 presents the flowchart of the work carried out. Prior to taking measurements, the preparation of the external wall was carried out by marking dimensions and applying a reflective smoothing coating to a section of the wall. After the installation of the temperature sensors, tests were conducted, and the results were thoroughly analyzed and corrected, taking into account factors that could affect the disturbances in the sensor readings.

The building on which the analyses were conducted was constructed in 2010 for technical purposes of the farm with a square footprint of 6×16.8 meters with a single-pitched roof, it has partial basement and has not been insulated. The external structural wall, on which the measurements were conducted, faces north-east, with internal room dimensions of 5.5×3.0 meters, and a total height at the peak of 7.5 meters. The external vertical barrier of the reference building is constructed from 0.24-m thick aerated concrete blocks. The room where the internal measurement was conducted is shown in Figure 2a, while a section of the external wall with the designated area for placing thermal insulation with and without a reflective coating is presented in Figure 2b.

The experiment was carried out using a Fluke 1586A SUPER-DAQ Precision Temperature Scanner (Fig. 3a), a multi-channel temperature data logger, in which the measurement channels were

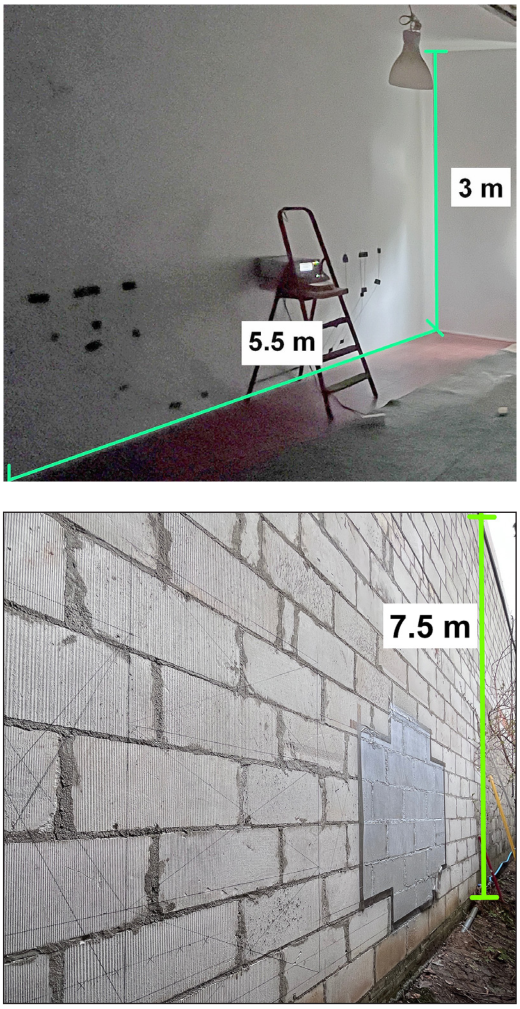

Figure 2. View of the tested wall with marked dimensions a) from the inside, b) from the outside

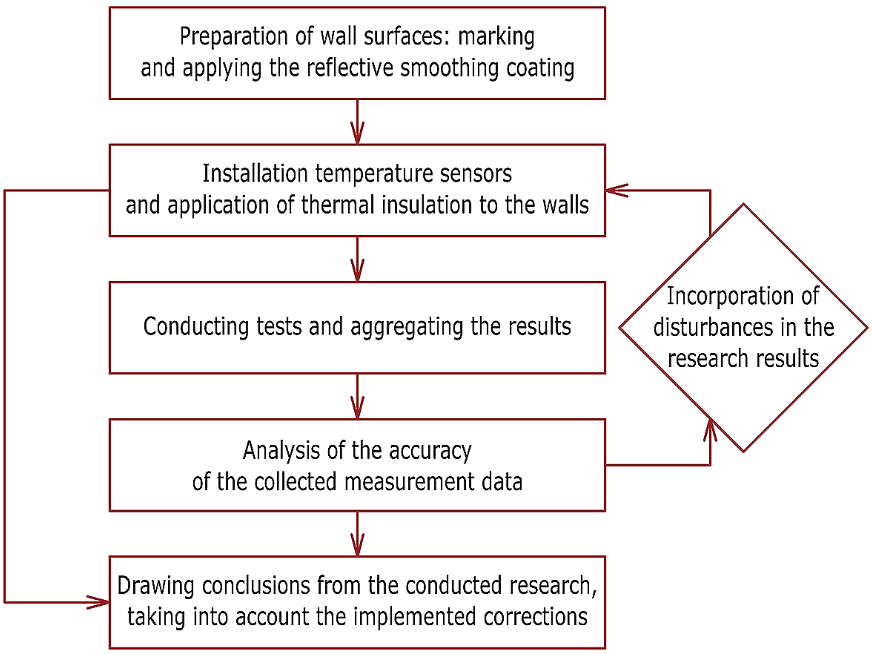

Figure 1. Flowchart of the work carried out

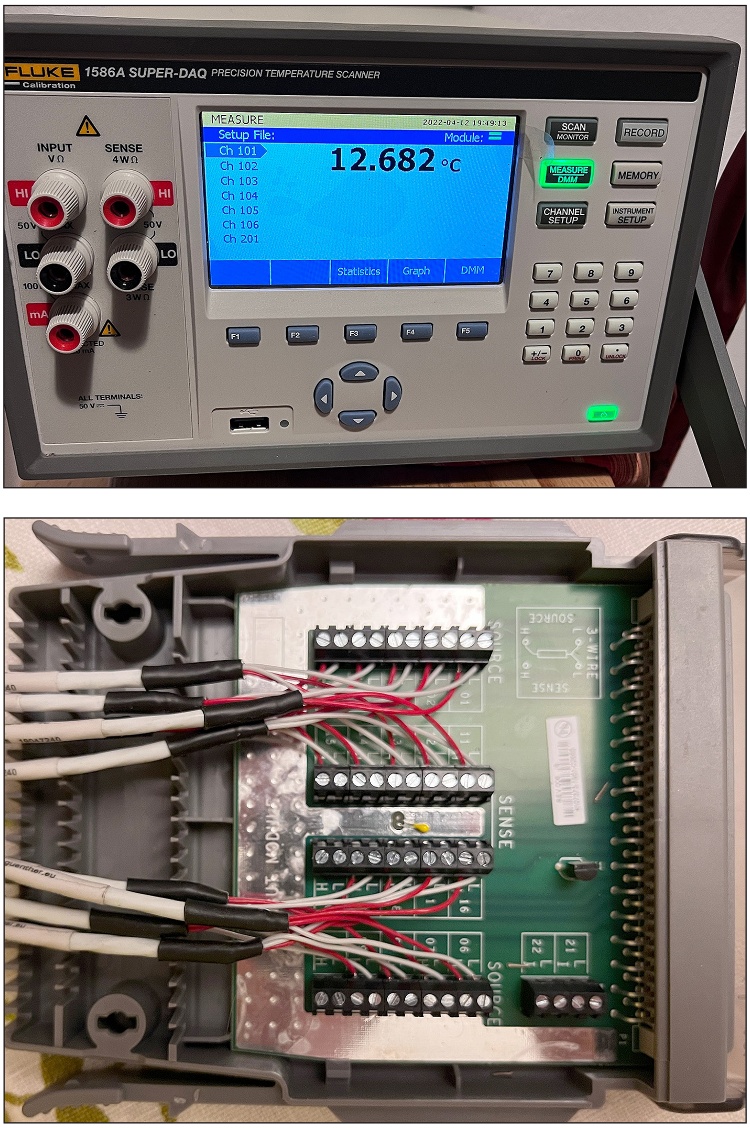

Figure 3. View of the tested wall with marked dimensions a) from the outside, b) from the inside

expanded using High Capacity Input Module card (Fig. 3b). Twenty sensors connected with integrated four-wire Pt100 cables were placed in the area of the wall under investigation and connected to the data logger (Fig. 3b, 4, 5).

As part of the experiment, thermocouples were placed in the walls after which thermal insulation was stuck on the adhesive mortar. Figure 4 shows a horizontal cross-section of the wall at the location where the thermocouples were placed in the air layer and the adhesive layer. In the second model, before applying polystyrene, the outer side of the wall was covered with a reflective and smoothing coating, which was silver-colour enamel, cast off from aerosol (Fig. 5). The study of heat transport in vertical multilayer walls under real conditions was conducted in accordance with the guidelines outlined in ISO 9869-1:2014 [31] and ISO 9869-2:2014 [32].

Before the installation of thermal insulation, four thermocouples were mounted at the locations marked for the arrangement of reference plates according to on the exterior side of the barrier: two at the areas of adhesive mortar application and two at the locations of the air gap. On the opposite side of the barrier, temperature sensors were positioned and marked in exactly the same locations. This arrangement allowed for the sensors to be placed in corresponding positions on both sides of the structural wall (Figure 4, 5). The ambient external temperature was recorded from two probes placed 0.3 m away from the reference plates' planes (channels Ch109 and Ch110). The internal temperature was measured by a probe (channel Ch209 and 210) located at the same height as the other sensors, 0.3 m away from the wall.

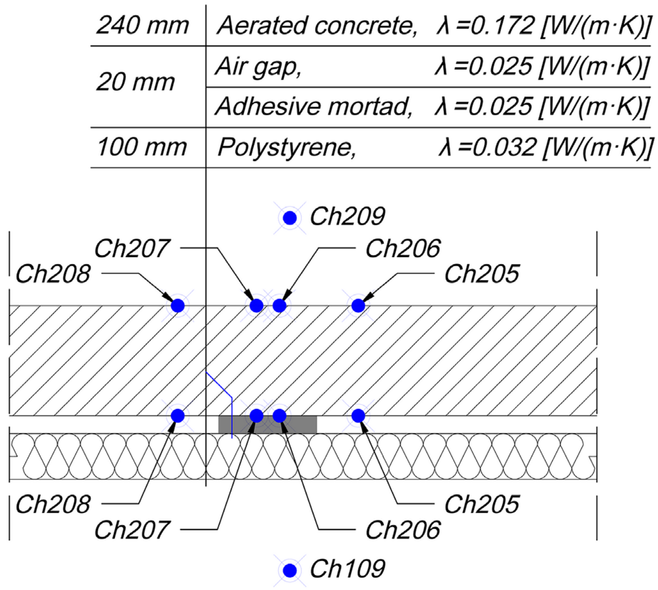

Figure 4. The distribution of temperature sensors in the analysed wall

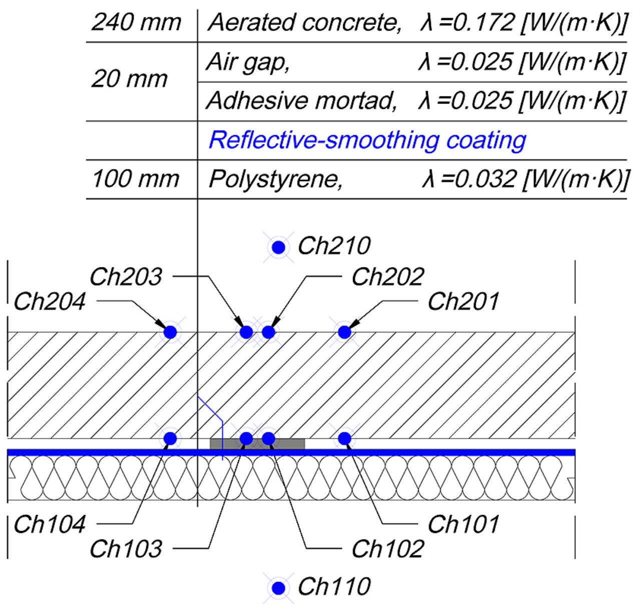

Figure 5. The distribution of temperature sensors in the analysed wall covered by the reflective-smoothing coating

RESULTS AND DISCUSSION

The measurements were carried out in April 2022, the total measurement time was 445 hours and 50 minutes, and records from all 20 channels were collected simultaneously at 60-second intervals (steps). These measurements, aimed at verifying the developed solutions in real conditions, took much longer due to changing weather conditions and the need to equalize the temperature inside the room. A total of 508250 records from 20 measurement channels were recorded. The ISO 9869:2014 standards [31][32] defines the representative period of conducting field thermal resistance tests in building partitions as 72 hours, thus measurement range between 8260 and 12580 readings was selected for the analysis, due to the stabilization of temperature and the absence of anomalies on both sides of the partition.

Indoor temperature measurements

Figure 6 shows the temperature measurement profile (Ch209) on the internal side

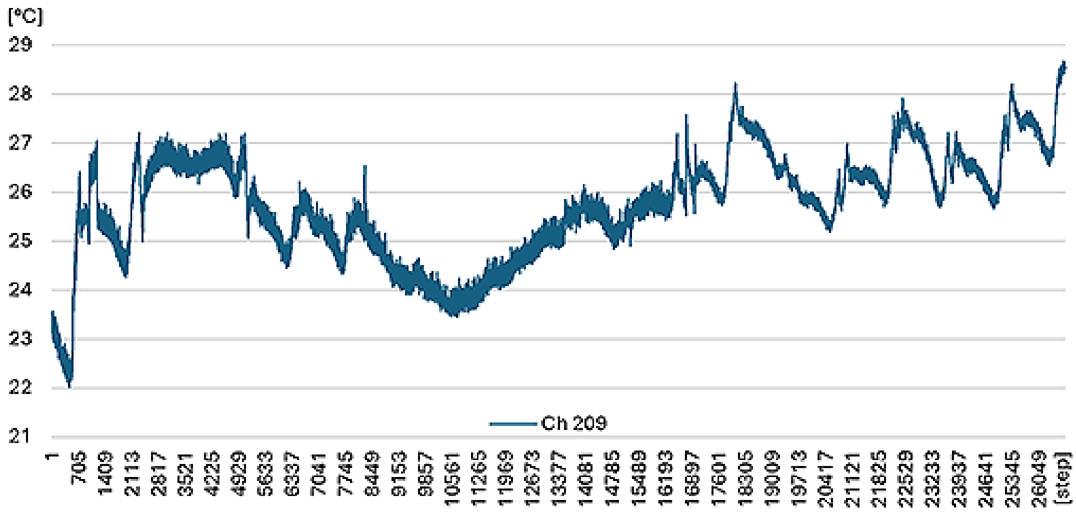

Figure 6. Temperature measurement profile (Ch209) on the internal side of the partition

of the wall, while Figure 7 shows recorded temperature measurement profile (Ch109, Ch110) on the external side of the wall. The graphs present the recorded profiles from both sides of the partition over the full-time range, i.e., over 19 days.

Figure 7 shows the temperature waveform recorded on the outer side of the partition. In this case, the ambient temperature sensors correctly recorded the values from the two external channels, which is important in changing weather conditions. The Ch109 channel collected information from the sensor located opposite the uncoated part of the wall, while the Ch110 channel collected information from the sensor in front of the wall with a reflective and smoothing coating applied. Despite the installation of two ambient temperature sensors, only one channel is visible on the reading from the internal side (Fig. 4), which prompted the researchers to verify the measuring device. As a result of the verification of the test bench, it turned out that the temperature sensor was damaged during assembly or service work, which resulted in a wrong reading. The temperature sensors were correctly installed before the commencement of the study. However, during the experiment, the tip of the thermocouple was damaged, as shown in Figure 8. This damage resulted from the thermocouple detaching from its mounting clips and subsequently striking the ground. The measuring device does not have the ability to control the course of measurements remotely and set alarms to notify the researcher of anomalies in real time. Nevertheless, the test

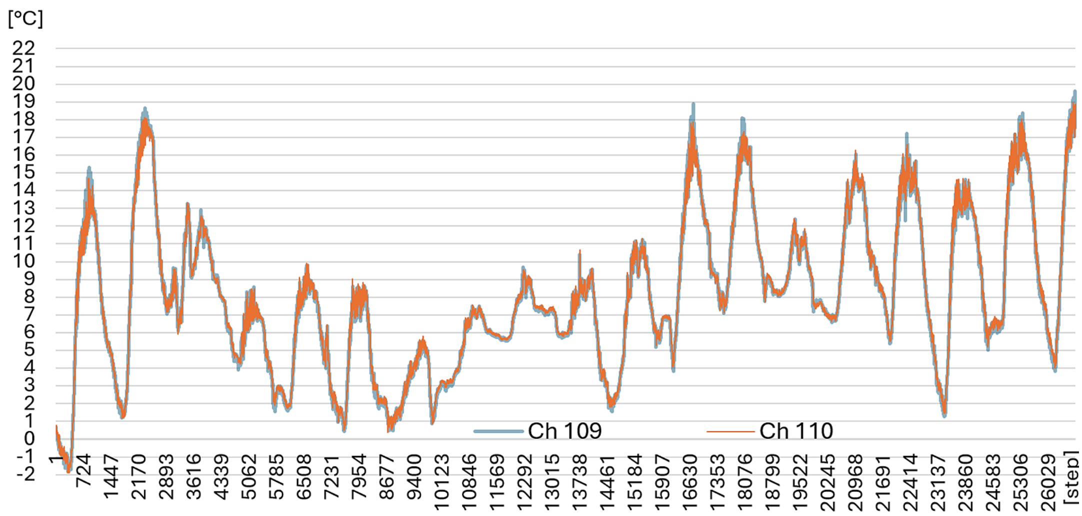

Figure 7. Temperature measurement profile (Ch109, Ch110) on the external side of the partition

Figure 8. Defective, damaged during the experiment Pt100 temperature sensor

results are considered to be correct, because the conditions in the room were constant and the facility protects them well from weather conditions. Hence, the recorded temperature values determining the temperature in the room on the basis of readings from one measurement channel are fully sufficient and does not require compensation.

Outdoor temperature measurements

Recorded temperature values are presented in Figure 9, with the graphical representation of the individual channels, where x-axis represents consecutive 60-second intervals (steps), and the y-axis shows the temperature range in degrees Celsius. After analysing the results from the selected 72-hour period and graphically representing the recorded values, a certain anomaly was observed in the area not covered by the reflective-smoothing coating, specifically in channels Ch101–Ch104. Although the thermocouples labelled as Ch102 and Ch103 were placed in close proximity to each other (50 mm) in the area covered with adhesive mortar, the readings from channel Ch103 significantly deviated from Ch102. This discrepancy necessitated a detailed analysis by the researcher of all factors, including verification of the measurement setup's accuracy and some review of the photographic documentation conducted during the experiment's preparation phase.

In Figure 9, thermocouples from channels Ch101 – Ch104 can be seen embedded in the structural layer before the application of adhesive mortar and thermal insulation in the form of polystyrene boards. The authors identified the placement of the measurement sensor in a location prone to erroneous temperature readings in this area as the cause of the anomaly. In the image (Fig. 10), the detail labelled "A" shows thermocouple Ch103 positioned very close to the joint, just 4 mm from the connection

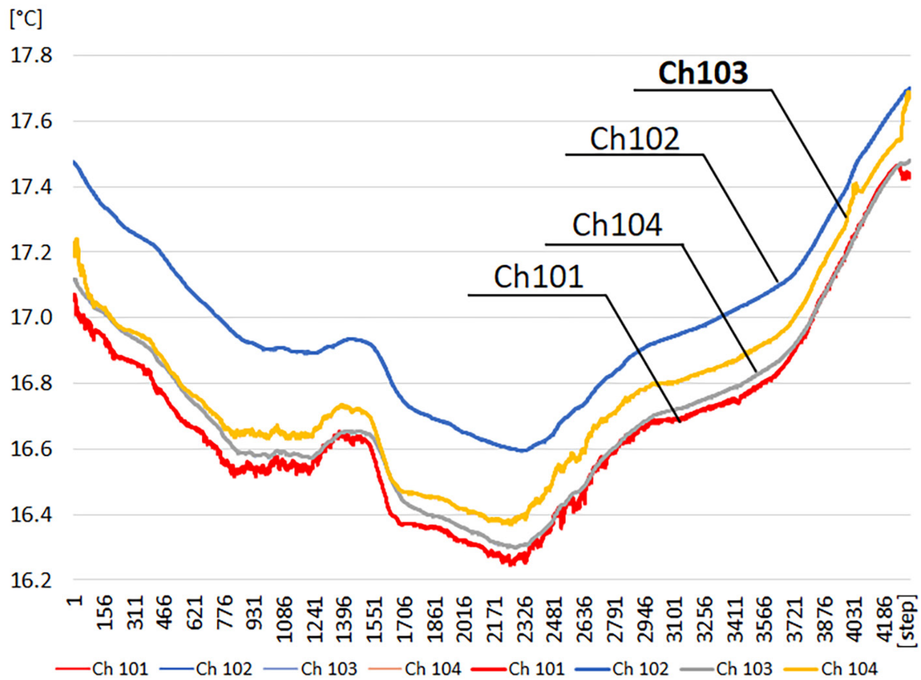

Figure 9. Measurement of the external wall temperature in the area not covered by the reflective-smoothing coating, during the representative 72-hour period

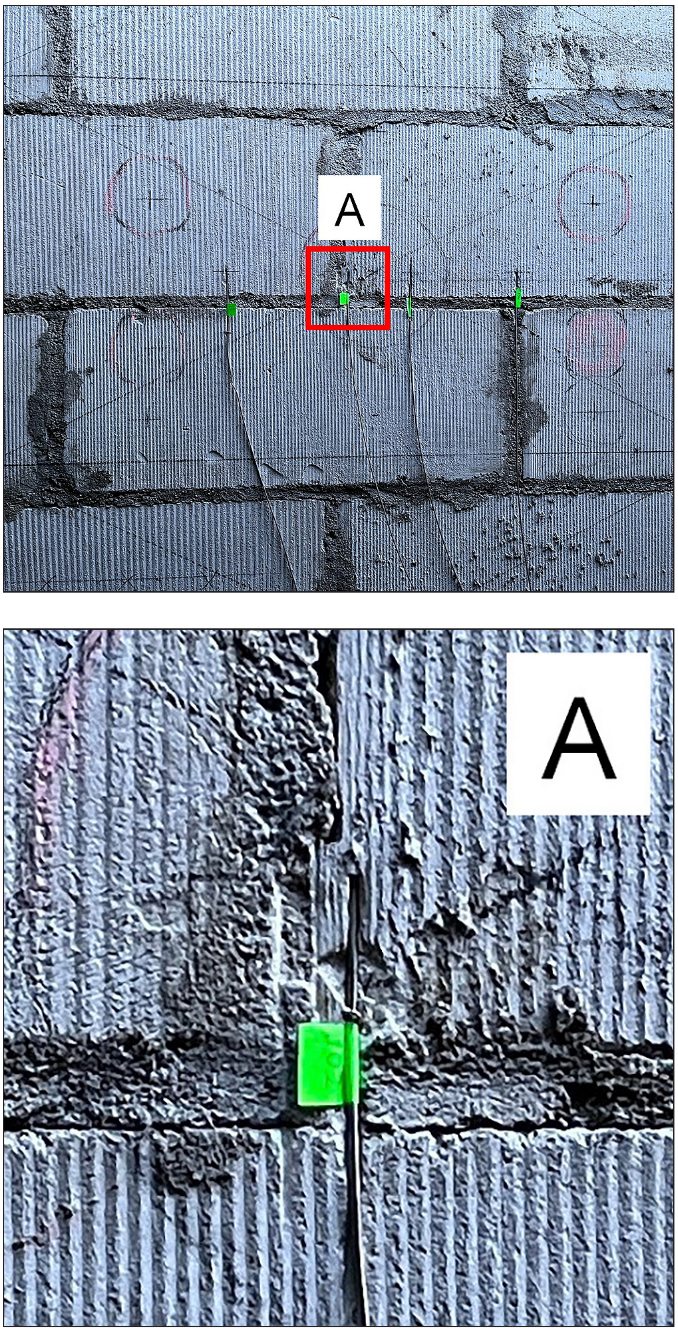

Figure 10. Thermocouples from measurement channels Ch101-Ch104 placed on the exterior side of the wall in the area not covered by the reflective-smoothing coating.

between the aerated concrete blocks. The laboratory-measured thermal conductivity coefficient of the block in an air-dry state is λ = 0.17 W/(m·K), while for the masonry mortar, it is λ = 0.34 W/(m·K). Thus, placing the thermocouple at the interface of two materials with different λ coefficients, densities, and porosities resulted in the disruption of accurate readings.

To verify the actual heat transport process in the measurement area of channel Ch103, the authors worked on identifying correlations between channels Ch101-Ch104 and the corresponding channels located in the area covered with the coating. As a result of implementing these correlations between the data from these measurement series, a graph was generated that likely represents the accurate temperature changes in channel Ch103 during the experiment (Fig. 11). This form of compensation, derived from the observed relationships between channels, can be effective, but it requires considerable effort to identify and adjust the measurements.

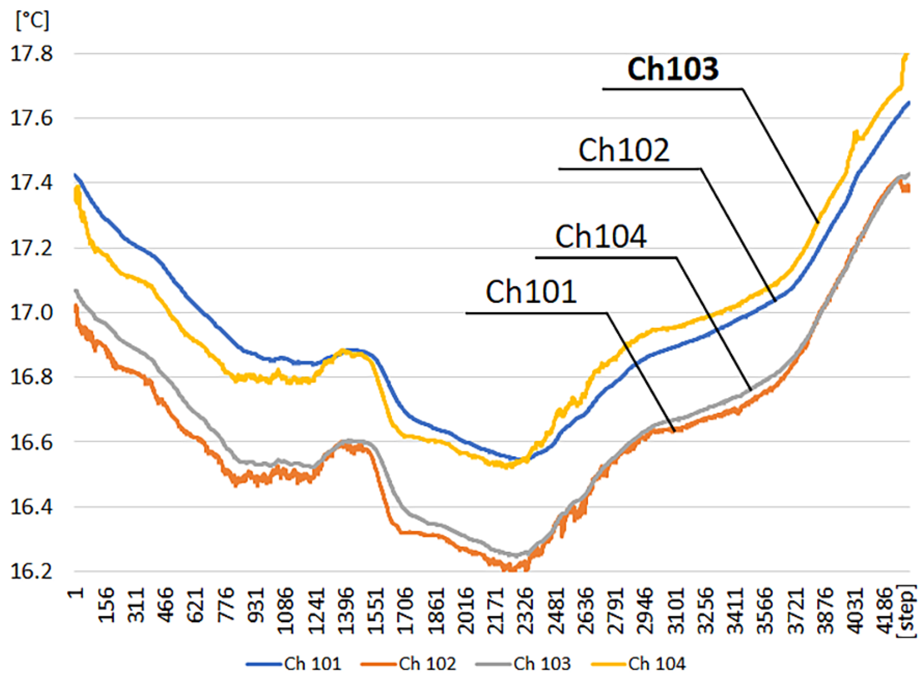

Figure 11. Measurement of the wall temperature in the area not covered by the reflective-smoothing coating, during the representative 72-hour period with values for channel Ch103 plotted after analysing the correlations between channels

CONCLUSIONS

The basic conclusion from the presented measurement results and their analysis is that this form of compensation, derived from the observed relationships between channels, is effective, but it requires considerable effort to identify and adjust the measurements. Authors of the article have conducted previous research using tools for modeling heat transfer simulations and have performed studies under laboratory conditions, where such measurement errors did not occur. Thus, the measurement of heat in multilayered walls enabled the drawing of conclusions:

The first measurement disturbance described in the study is related to the thermocouple malfunction and could have been eliminated in the initial phase of measurements. Therefore, it is advisable to implement remote monitoring of field research results, including internet connectivity. This is particularly important in long-term field studies. Without online diagnostic tools, compensation or repetition of the test will be required

In the second case, a deviation of just 0.2 °C was recorded resulting from the displacement of the measurement point, while the temperature amplitude on the external side during the experiments reached approximately 21 °C. In this case, when the reading is recorded simultaneously by 10 channels in short 60-second intervals, it is difficult to detect and requires algorithms capable of verifying the accuracy of the readings. Ensuring proper research conduct would crucially depend on the ability to verify the sensors' positions before applying the insulation layer. Otherwise, interference with the test setup could lead to its destruction. Hence, the development of modules integrated into measurement devices and systems, equipped with machine learning software, would be highly significant for detecting disturbances.

Two sources of measurement errors presented in the article – one caused by a sensor malfunction and the other by placement in a thermal bridge zone – may have led to misinterpretation of the results. Noticing these irregularities requires significant attention and extensive experience from the researcher, which still does not guarantee correct interpretation due to the overwhelming amount of data to analyze.

The conducted research demonstrates that performing heat analyses under in-situ conditions can be subject to measurement uncertainty for various reasons. Therefore, it is crucial to validate results by accounting for variable environmental conditions and potential measurement disturbances.

Error verification and proper interpretation of results can be supported by the application of machine learning tools; however, the challenge remains in learning the initial state, which is particularly difficult under variable real-world conditions during in-situ testing. In a study addressing the same problem developed by a team of researchers Xi B. at al. proposed a systematic approach to solving this issue, which could be implemented in the analysis of heat transfer phenomena in multi-layered walls. This approach verifies the accuracy of the simulation results by using the heat flux value as an index. It dynamically accounts for the influence of solar radiation and the heat transfer coefficients on both the inner and outer surfaces of the wall. Based on this approach, authors plan to further develop their research on reducing in situ-measurement result disturbances through the application of machine learning and artificial intelligence methods to analyse results and identify correlations within large datasets obtained from the sensors of the multi-channel temperature recorder.

REFERENCES

1. European Commission A Roadmap for moving to a competitive low carbon economy in 2050 Brussels, Belgium, 2011.
2. Ballarini I., Corrado V., Madonna F., Paduos S., Ravasio F., Energy refurbishment of the Italian residential building stock: energy and cost analysis through the application of the building typology, Energy Policy 2017; 105: 148–160,
3. Paśnikowska-Łukaszuk M., Wójcicka-Migasiuk D., Wośko E. Daily analysis of changes taking place in heat exchangers used in combined heat and power plants. Advances in Science and Technology Research Journal 2022; 16(6): 258–266,
4. Urzędowski A., Zaburko J., Gleń P., Łagód G., Numerical and Experimental Investigation of the Influence of External Wall Moisture on Building Temperature Distributions, Advances in Science and Technology Research Journal 2021; 15(3): 297–308,
5. Mikušová D., Suchorab Z., Paśnikowska-Łukaszuk M., Zaburko J., Trnik A. Applying the machine learning method to improve calibration quality of time domain reflectometry measuring technique. Advances in Science and Technology Research Journal 2024; 18(3): 270–279.
6. Paśnikowska-Łukaszuk M., Wlazło-Ćwiklińska M., Zubrzycki J., Suchorab Z. Comparison of measurement possibilities by non-invasive reflectometric sensors and invasive probes, 2023.
7. Sharma S., Pany C., Suresh R., Ahamed S.S. E-Seal in a typical convergent–divergent (CD) nozzle for a liquid engine BT. Advances in Thermal Engineering, G. Choubey, S. Tripathi, V. K. Singh, and P.M.V Subbarao (Eds.), Singapore: Springer Nature Singapore 2024: 151–164.
8. Sharma S., Pany C., Suresh R., Ahamed S., Krishnadasan C.K., Spiral wound gasket in a typical liquid engine convergent-divergent nozzle BT - Advances in Thermal Sciences, V.K. Singh, G. Choubey, and S. Suresh, Eds., Singapore: Springer Nature Singapore 2023: 187–201.
9. Kosiński P., Brzyski P., Suchorab Z., Łagód G. Heat losses caused by the temporary influence of wind in timber frame walls insulated with fibrous. Materials 2020.
10. Urzędowski A., Styczeń J., Wójcicka-Migasiuk D. Analysis of thermal properties and heat loss in construction and isothermal materials of multilayer building walls, Advances in Science and Technology Research Journal 2017; 11(2): 33–37.
11. Majerek D., Sędzielewska E., Paśnikowska-Łukaszuk M., Łazuka E., Suchorab Z., Łagód G. Automatic image analysis method as a tool to evaluate the anisotropy of autoclaved aerated concrete for moisture and heat transport 2024.
12. Chwieduk D. A., Some aspects of energy efficient building envelope in high latitude countries, Solar Energy 2016; 133: 194–206.
13. Evaluation of measurement data — Guide to the expression of uncertainty in measurement, 2008.
14. Kubiczek K., Kampik M., Grzenik M., Analysis of DC reversal error of the calorimetric thermal voltage converter, Measurement 2021; 168: 108439.
15. Taylor J. Wstęp do analizy błędu pomiarowego. Warszawa: Wydawnictwo Naukowe PWN, 1995.
16. Li F., Zuo W., Zhou K., Li Q., Huang Y., Zhang G., State-of-charge estimation of lithium-ion battery based on second order resistor-capacitance circuit-PSO-TCN model. Energy 2024; 289: 130025.
17. Huang Y. et al. A high constancy and noise suppression voltage shift generator in SEIR-based BIST circuit for ADC linearity test. Microelectronics Journal 2024; 151: 106341.
18. Lisowski M. Podstawy metrologii. Wrocław, 2011.
19. Słoma J., Szczygieł I., Sachajdak A., Modelling of thermal phenomena in electric arc during surfacing, Archives of Civil and Mechanical Engineering 2011; 11(2): 437–449.
20. Sachajdak A., Słoma J., Szczygieł I. Thermal model of the gas metal arc welding hardfacing process. Applied Thermal Engineering 2018; 141: 378–385.
21. Sachajdak A., Lappalainen J., Mikkonen H. Dynamic simulation in development of contemporary energy systems – oxy combustion case study. Energy 2019; 181: 964–973.

22. Kou Z., Wu R., Wang Q., Li B., Li C., Yin X. Heat transfer error analysis of high-temperature wall temperature measurement using thermocouple. Case Studies in Thermal Engineering 2024; 59: 104518,
23. Barnat-Hunek D., Lagod G., Klimek B., Evaluation of the contact angle and frost resistance of hydrophobised heat-insulating mortars with polystyrene, vol. 1866. 2017.
24. 1225 Dz.U. 2022 poz., Obwieszczenie Ministra Rozwoju i Technologii z dnia 15 kwietnia 2022 r. w sprawie ogłoszenia jednolitego tekstu rozporządzenia Ministra Infrastruktury w sprawie warunków technicznych, jakim powinny odpowiadać budynki i ich usytuowanie.
25. PN-EN ISO 6946:2017. Komponenty budowlane i elementy budynku Opór cieplny i współczynnik przenikania ciepła Metoda obliczania.
26. PN-EN ISO 13789:2017-10. Thermal performance of buildings - transmission and ventilation heat transfer.
27. PN-EN ISO 12524:2003. Building materials and products.
28. Bienvenido-Huertas D., Moyano J., Marín D., Fresco-Contreras R. Review of in situ methods for assessing the thermal transmittance of walls, Renewable and Sustainable Energy Reviews 2019; 102: 356–371.
29. Ha T. T. et al., Measurement prototype for fast estimation of building wall thermal resistance under controlled and natural environmental conditions, Energy and Buildings 2022; 268: 112166. https://doi.org/10.1016/J.ENBUILD.2022.112166.
30. François A., Ibos L., Feuillet V., Meulemans J., Novel in situ measurement methods of the total heat transfer coefficient on building walls, Energy and Buildings 2020; 219: 110004,
31. ISO 9869-1:2014, Thermal insulation – Building elements – In-situ measurement of thermal resistance and thermal transmittance – Part 1: Heat flow meter method.
32. ISO 9869-2:2014, Thermal insulation – Building elements – In-situ measurement of thermal resistance and thermal transmittance – Part 2: Infrared method for frame structure dwelling.
33. Khalifa A.J.N., Marshall R.H., Validation of heat transfer coefficients on interior building surfaces using a real-sized indoor test cell, International Journal of Heat and Mass Transfer 1990; 33(10): 2219–2236.
34. Jayamaha S. E. G., Wijeysundera N. E., Chou S. K., Measurement of the heat transfer coefficient for walls, Building and Environment, 1996, 31(5): 399–407.
35. Pinheiro Ramos N., Delgadillo Buenrostro L. Metrevelle Marcondes de Lima e Silva S., Gosselin L., Inverse estimation of the annual heat flux through the internal surface of a multilayer wall in an occupied prefabricated house from field measurements, International Communications in Heat and Mass Transfer 2024; 158: 107872.
36. Choi J.S., Kim C., Jang H., Kim E.J. In-situ evaluation of window-wall joint performance using numerical models and thermal images. Case Studies in Thermal Engineering 2023; 45: 102988.
37. Zhang D., Zhan C., Chen L., Wang Y., Li G. An in-situ detection method for assessing the thermal transmittance of building exterior walls using unmanned aerial vehicle–infrared thermography (UAV-IRT), Journal of Building Engineering 2024; 91: 109724.
38. Xu B., Cheng Y. xia, Chen X. ni, Xie X., Ji J., Jiao D. Sheng, Error correction method for heat flux and a new algorithm employed in inverting wall thermal resistance using an artificial neural network: Based on IN-SITU heat flux measurements, Energy, 2023, 282: 128896.
39. Li W., Zhang G., Yang D., Comparative study for flow condensation heat transfer in horizontal enhanced tubes based on machine learning. International Journal of Heat and Mass Transfer 2024; 224: 125330.
40. Vohra K., Vodonos A., Schwartz J., Marais E.A., Sulprizio M.P., Mickley L.J., Global mortality from outdoor fine particle pollution generated by fossil fuel combustion: Results from GEOS-Chem, Environmental Research 2021; 195: 110754.
41. Woroniak G., Piotrowska-Woroniak J. Effects of pollution reduction and energy consumption reduction in small churches in Drohiczyn community, Energy and Buildings 2014; 72: 51–61.
42. Tzoulis T., Kontoleon K.J. Thermal behaviour of concrete walls around all cardinal orientations and optimal thickness of insulation from an economic point of view. Procedia Environmental Sciences 2017; 38: 381–388.
43. Siddique N., Paheding S., Elkin C.P., Devabhaktuni V., U-Net and Its Variants for Medical Image Segmentation: A Review of Theory and Applications, IEEE Access, 2021; 9: 82031–82057.
44. Liu Z., Mao H., Wu C.Y., Feichtenhofer C., Darrell T., Xie S., A ConvNet for the 2020s, Proceedings of the IEEE Computer Society Conference on Computer Vision and Pattern Recognition,. 2022: 11966–11976.
45. Wightman R., Touvron H., Jégou H., ResNet strikes back: An improved training procedure in timm 2021: 1–22.
46. Liu Z. et al. Swin transformer: hierarchical vision transformer using shifted windows, in 2021 IEEE/CVF International Conference on Computer Vision (ICCV), 2021.
47. Waqas A., Araji M. T., Machine learning-aided thermography for autonomous heat loss detection in buildings, Energy Conversion and Management 2024; 304: 118243.